APPLICATION OF LOW PLASTICITY BURNISHING (LPB) TO IMPROVE THE CORROSION FATIGUE PERFORMANCE AND FOD TOLERANCE OF ALLOY 450 STAINLESS STEEL

N. Jayaraman (njayaraman@lambda-research.com)
Paul S. Prevéy (pprevey@lambda-research.com)

Lambda Research
5521 Fair Lane, Cincinnati, OH 45227–3401

ABSTRACT

The potential corrosion fatigue performance benefit of applying low plasticity burnishing (LPB) to alloy 450 stainless steel (UNS S45000) was investigated. Damage tolerance and aggressive corrosion fatigue were simulated. The LPB process was optimized to produce nominally 0.035 in. (0.9 mm) of compression in the alloy 450 stainless steel. LPB increased the HCF endurance limit for corrosion fatigue (in an acidic salt solution environment) by nominally 60%, from 100 ksi (~700 MPa) to nearly 160 ksi (~1100 MPa). LPB processing of bars with EDM notching to a depth of 0.01 in. (0.25 mm) (to simulate erosion/foreign object damage (FOD)) followed by corrosion fatigue increased the corrosion fatigue strength by a factor of 8, from 15 to 125 ksi (~100 to 860 MPa). Increased FOD size up to 0.03 in. (0.75 mm) only nominally decreased the corrosion fatigue performance. LPB surface enhancement provides substantially improved corrosion fatigue life and damage tolerance in alloy 450 stainless steel through deep surface compressive residual stresses.

Mechanistically, the effect of corrosion and FOD resulted in early crack initiation and growth, and dramatically decreasing the fatigue performance. Despite the existence of similar corrosion conditions, the deep compressive surface residual stresses from LPB treatment helped to mitigate the individual and synergistic effects of corrosion fatigue and FOD.

Keywords: Residual Stresses, Surface Enhancement, Corrosion Fatigue, Low Plasticity Burnishing (LPB), Foreign Object Damage (FOD)

INTRODUCTION

Corrosion is generally understood to be a chemical/electrochemical process involving the attack of the base metal/alloy by a liquid (often aqueous), or gaseous environment. Hence most methods to protect against corrosion involve somehow chemically altering the base metal, the environment, or the interface between the two. Such protections have proved to be very useful in numerous engineering systems. However, the structural integrity of engineering structures operating in conditions where both mechanical fatigue and corrosion act synergistically continues to provide a challenge for the engineering community. Corrosion fatigue is increasingly identified to be a critical problem in numerous engineering components.

Introduction of residual compressive stresses in metallic components has long been recognized[1-4] to lead to enhanced fatigue strength. For example, many engineering components have been shot-peened or cold worked with fatigue strength enhancement as the primary objective or as a by-product of a surface hardening treatment like carburizing/nitriding, physical vapor deposition, etc. Over the last decade, other examples of the former type of treatment like LPB,[5] laser shock peening (LSP),[6] and ultrasonic peening

have emerged. All of these surface treatment methods have been shown to benefit fatigue prone engineering components to different degrees.

LPB has been demonstrated to provide a deep surface layer of high magnitude compression in various aluminum, titanium, nickel based alloys and steels. Thermal and mechanical stability are obtained when deep compression is achieved with minimal cold work of the surface. The deep stable compressive residual stress state on the surface of these materials has been shown to be effective in mitigating fatigue damage due to FOD,[7-9] fretting,[10-11] and pitting/corrosion.[12-15] The LPB process can be performed on conventional CNC machine tools at costs and speeds comparable to conventional machining operations such as surface milling.

The main goal of this research is to investigate the effectiveness of a compressive surface residual stress state imparted by the LPB process upon the adverse effects of corrosion fatigue, FOD, and pitting damage in alloy 450 stainless steel.

EXPERIMENTAL PROCEDURE

Material and Heat Treatment

Alloy 450 stainless steel was procured in the form of forged bars, with an approximate size of 1.5 in. X 2 in. X 9 in. (38 mm X 50 mm X 225 mm). All bars were heat treated to the H1050 condition – i.e., solution treated at 1038 ºC for 1 hour, followed by a water quench, and aged at 566 ºC for 4 hours, followed by air cooling. The nominal composition and tensile properties of the heat-treated steel are as follows:

Chemical Composition: (All weight%) C-0.029%, Nb-0.72%, Cr-14.95%, Cu-1.73%, Mn-0.43%, Mo-0.79%, Ni-7.06%, P-0.019%, S-0.002%, Si-0.45%, Ti-<0.01%, Bal-Fe.

0.2% Y.S. = 155 ksi (1,070 MPa), UTS = 166 ksi (1,145 MPa), % Elong. = 18.8, %RA = 68.6

LPB Processing

LPB process parameters were developed by Surface Enhancement Technologies, LLC, (SET) for thick sections of alloy 450 stainless steel using proprietary methods to impart the greatest depth and magnitude of residual stress with minimal cold work. CNC control code was modified to allow positioning of the LPB tool in a series of passes along the gage section while controlling the burnishing pressure to develop the desired magnitude of compressive stress with relatively low cold working. Figure 1a shows a thick section fatigue specimen in the process of being low plasticity burnished in the four-axis manipulator on the CNC milling machine. Figure 1b shows a thick section fatigue specimen with a LPB processed top surface.

HCF Specimen Processing

Thick section fatigue specimens with nominal dimensions of 1.25 in X 0.375 in. X 8 in. (31.25 mm X 9.375 mm X 200 mm) were finish machined out of these bars by low stress grinding. A typical fatigue specimen is shown in Figure 1c, which has a trapezoidal cross section in the gage region. This special design enables the testing of surface treated specimens with deep compressive residual stresses on the surface. The trapezoidal cross section HCF sample with compressive surface residual stresses was designed to force fatigue failures to initiate in the gage section under 4-point bend loading.

Two sets of eight samples were fatigue tested after low stress grinding (LSG) and another two sets after LPB processing. The entire gage region was LPB processed with the optimal parameters chosen as discussed above. To simulate the effects of FOD, a semi-elliptical surface notch depth of a_o = 0.01 in. (0.25 mm) and surface length of $2c_o$ = 0.06 in. (1.5 mm) was introduced by electrical discharge machining (EDM). One set each of specimens with LSG finish and LPB finish were tested with the EDM notch, and another set without the EDM notch. Additionally, in an attempt to find the limiting FOD depth that the LPB treated surfaces could tolerate, a few LPB treated specimens were

tested with 0.02 in. (0.5 mm) and 0.03 in. (0.75mm) deep EDM notches.

High Cycle Corrosion Fatigue Testing

All high cycle fatigue tests were performed under constant amplitude loading on a Sonntag SF-1U fatigue machine. A photo of the fatigue test setup is shown in Figure 1d. Fatigue testing was conducted at ambient temperature (~72F) in four-point bending mode. The cyclic frequency and load ratio, R, were 30 Hz and 0.1, respectively. Tests were conducted to the event of specimen fracture or until a "run-out" life of 2.5 x 10^6 was attained. Run-out specimens were subsequently re-tested to fracture at a stress at least 20 ksi above the stress level at which run-out occurred. For analysis purposes, such re-tests were regarded as virgin tests and results were included thus in S-N results. Cycling was terminated upon separation of the sample or when displacement resulting from severe cracking exceeded equipment limits. Specimens from tests terminated for the latter reason were subsequently broken by hand to permit direct observation of fracture surface details.

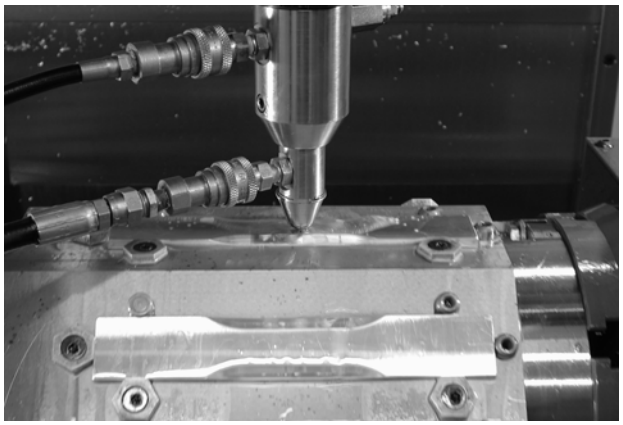

Figure 1a: A set of 8 thick section specimens being LPB processed in a 4-axis CNC milling machine.

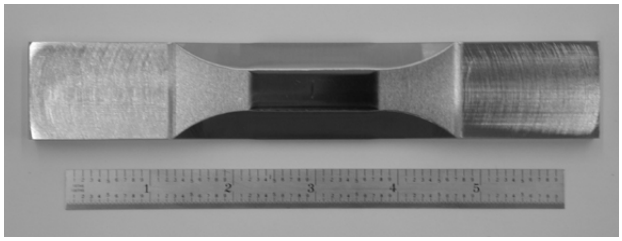

Figure 1b: The LPB treated surface patch in the gage section of a thick section specimen.

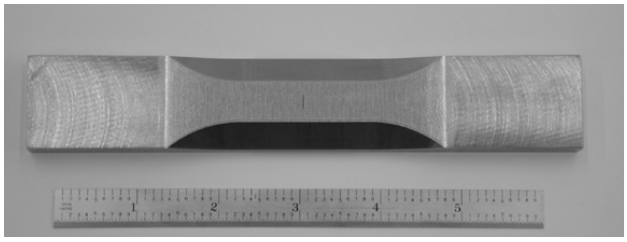

Figure 1c: Photograph of a typical thick section specimen

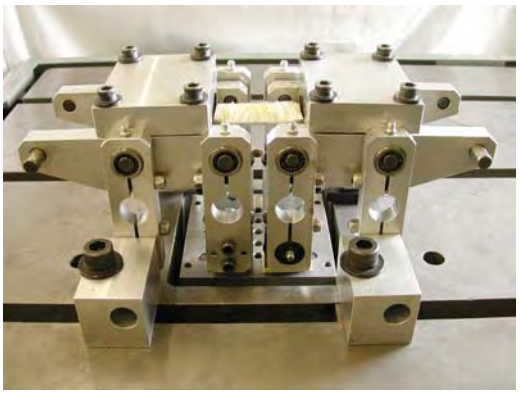

Figure 1d: A specimen mounted in the 4-point bend fatigue test apparatus.

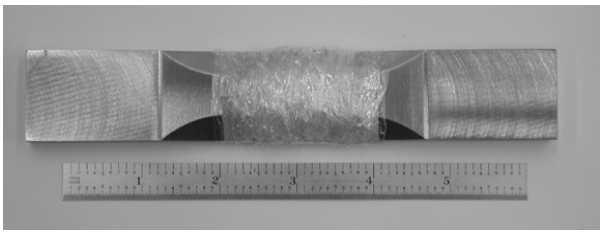

Figure 1e: A thick section specimen with the acidic salt solution soaked tissue papers wrapped around the gage section, ready for corrosion fatigue test.

All fatigue tests were carried out in an aqueous acid salt solution environment consisting of a 3.5

wt% NaCl salt solution with a pH of about 3.5. Samples were prepared by soaking filter papers with the solution, wrapping the soaked filter paper around the gage section of the fatigue test specimen, and sealing the entire gauge section with a plastic film. The solution pH was adjusted by adding a few drops of 1 molar solution of HCL. Figure 1e shows a specimen prepared for corrosion fatigue testing. Figure 1d shows the specimen mounted in the four-point bend fixture assembled for fatigue testing in a Sonntag SF-1U HCF testing machine.

Residual Stress Measurement

X-ray diffraction residual stress measurements were made at the surface and at several depths below the surface on LPB treated fatigue specimens. Measurements were made in the longitudinal direction in the fatigue specimen gage employing a $\sin^2\psi$ technique and the diffraction of chromium Kα1 radiation from the (211) planes of steel. The lattice spacing was first verified to be a linear function of $\sin^2\psi$ as required for the plane stress linear elastic residual stress model.[16-19]

Material was removed electrolytically for subsurface measurement in order to minimize possible alteration of the subsurface residual stress distribution as a result of material removal. The residual stress measurements were corrected for both the penetration of the radiation into the subsurface stress gradient[20] and for stress relaxation caused by layer removal.[21] The value of the x-ray elastic constants required to calculate the macroscopic residual stress from the strain normal to the (211) planes of steel were determined in accordance with ASTM E1426-91.[22] Systematic errors were monitored per ASTM specification E915.

Fractography

Following fatigue testing, each specimen was examined optically at magnifications up to 60X to identify fatigue origins and locations thereof relative to the specimen geometry. Pictures were taken with a Nikon 990 digital camera through a Nikon Stereoscopic microscope at 15x. A representative photograph of a typical failure for each specimen group was obtained. A few selected specimens were also examined under a Cambridge S90B SEM.

RESULTS AND DISCUSSION

Residual Stress Distributions

The residual stress distributions measured as a function of depth are presented in Figure 2. Compressive stresses are shown as negative values, tensile as positive, in units of ksi (10^3 psi) and MPa (10^6 N/m^2).

Figure 2 shows the residual stress (RS) profiles for LPB processed specimens after fatigue testing. Surface compression is nominally -140 ksi (-965 MPa) and –175 ksi (-1,200 MPa) for the two specimens tested. Coincidentally, the surface shows maximum compression, which gradually decreases over a depth of about 0.035 in. (~0.9 mm) from the surface. In both specimens shown in Figure 2 fatigue cycling appears to have a minimal effect on the residual stresses; even fatigue cycling at a Smax of 195 ksi (1,345 MPa) in Specimen 12 seems to produce little relaxation of stresses near the surface.

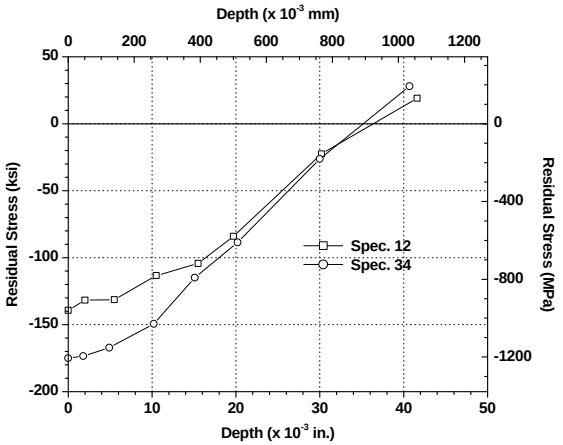

Figure 2. Residual stress distribution for two LPB processed (and fatigue tested) specimens.
Specimen #12 (LPB – no notch): S_{max} = 195 ksi (~1,345 MPa); N_f = 141,191 cycles
Specimen #34 (LPB + notch): S_{max} = 160 ksi (~1,100 MPa); N_f = 159,941 cycles

Corrosion Fatigue Performance

Figure 3 shows the corrosion fatigue performance of alloy 450 stainless steel (H1050) in the form of S-N curves. The baseline material (LSG) performance with and without the EDM notch is compared with similarly tested specimens with LPB treatment. The unnotched LSG condition shows a fatigue strength (endurance limit at about 10^7 cycles) of about 100 ksi (~700 MPa). It is obvious that the introduction of a semi-elliptical EDM notch of nominal size a_o = 0.010 in. (0.25 mm) and c_o = 0.030 in. (0.75 mm) drastically decreases the corrosion fatigue strength to about 10 ksi (~70 MPa). The fatigue lives at higher stresses show a corresponding decrease by over an order of magnitude.

In contrast, the unnotched set of LPB specimens show a fatigue strength of about 160 ksi (~1,100 MPa). The introduction of the EDM notch only marginally reduced the fatigue strength to a value of 125 ksi (860 MPa). It is particularly noteworthy that this fatigue strength of notched LPB specimens is much better than the unnotched LSG specimens. Additionally, the two data points for LPB specimens with semi-elliptical EDM notch of a_o = 0.020 in. (0.5 mm) and c_o = 0.060 in. (1.5 mm) tested at 120 ksi (~825 MPa) and 95 ksi (~655 MPa) show fatigue lives comparable to similarly tested LSG specimens, within the limits of experimental scatter. However, the LPB specimen with an EDM notch of a_o = 0.030 in. (0.75 mm) and c_o = 0.090 in. (2.25 mm) when tested at 120 ksi (~825 MPa) showed a substantial decrease in fatigue life

Fractography

Figures 4, 5 and 6 show SEM fractographs of unnotched LSG, LPB, and notched specimens, respectively. Figures 4a – c show the fracture features of an unnotched LSG specimen. It is evident from Figure 4a, that the fracture process involved multiple crack initiation from corrosion pits on the surface. As seen in Figure 4b, the corrosion pit formation was further aided by the presence of grind marks on the surface.

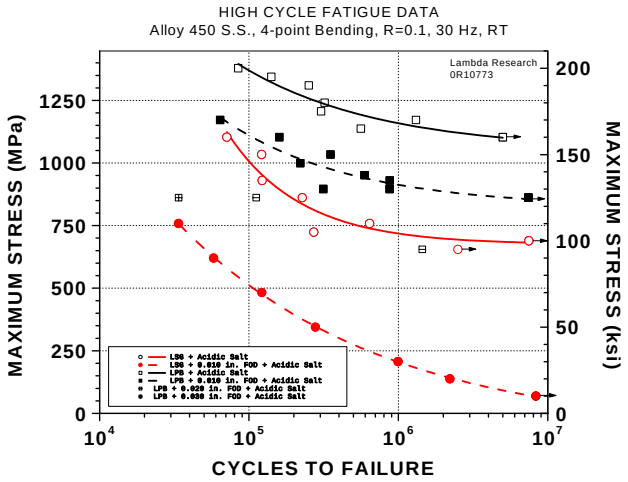

Figure 3. Corrosion fatigue results plotted in the form of S-N curves. Note that the LPB specimens substantially outperformed the LSG specimens.

Figure 4c shows the general crack growth process was by intergranular cracking. This crack growth process beyond the crack initiation region was observed in all specimens, independent of surface treatment. In contrast to Figure 4 for LSG, the LPB specimens generally showed no distinct crack initiation from the surface. Typically, crack initiation was observed to be below the LPB treated surface, as seen in Figure 5. This is indicative of the fact that the compressive residual stress from the LPB treatment was successful in mitigating crack initiation from the surface. These observations are further corroborated in Figures 6a and 6b where the fracture surfaces of notched specimens are compared. Again in these fracture surfaces, the LSG specimen in Figure 6a shows no particular feature associated with crack initiation and growth, i.e., no struggle for the fracture process, while the LPB specimen in Figure 6b shows the dark coloration beneath the notch, similar to that seen in Figure 5. Again the radial crack growth marks converge at a point below the notch thus indicating a sub-surface initiation.

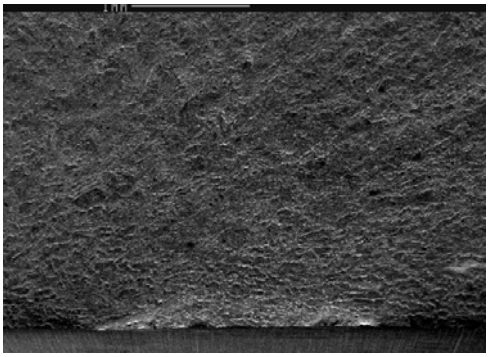

Figure 4a: Fracture surface showing multiple initiation sites.

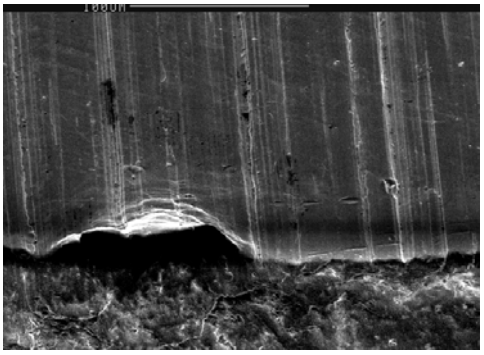

Figure 4b: Evidence of corrosion pitting attack along the grind marks and several deformed corrosion pits at one of the initiation sites.

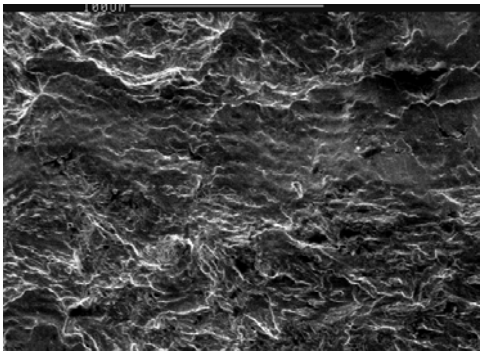

Figure 4c: Crack growth region showing intergranular cracking. Specimen #4. Smax = 110 ksi (~760 MPa), Nf = 641,792 cycles.

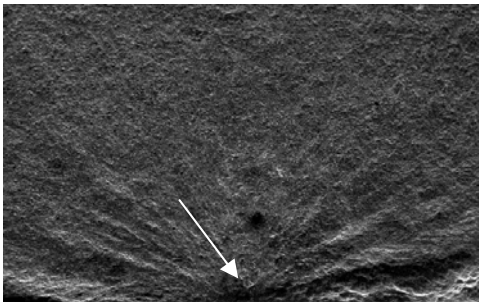

Figure 5: Fracture surface of a LPB treated specimen; the radial crack growth marks actually converge at a point roughly 0.5 mm below the specimen surface (arrow), indicating that the LPB treatment was successful in mitigating the corrosion-pit related crack initiation seen in Figure 1a. Specimen #21, Smax = 170 ksi (~1,170 MPa), Nf = 1,311,786cycles

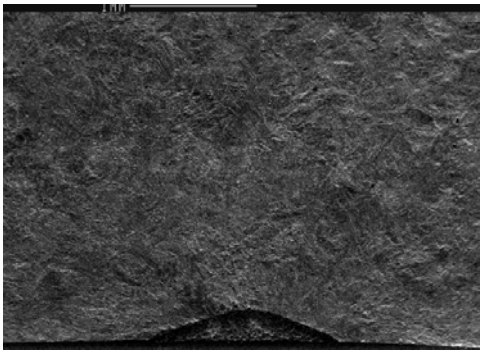

Figure 6a: Specimen #39, Smax = 20 ksi (~138 MPa), Nf = 2,211,712 cycles.

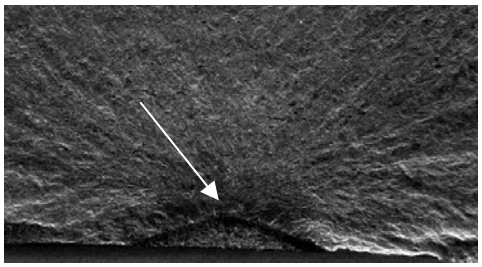

Figure 6b: Specimen #38, Smax =135 ksi (930 MPa), Nf = 875,204 cycles.

Figure 6a: Fracture surface of LSG specimen with EDM notch showing no particular indication of crack initiation, LPB specimen in 6b. shows evidence of crack initiation below the notch leading to radial crack growth marks on the fracture surface. The dark coloration below the notch is similar to that noticed near the crack origin in Figure 5.

DISCUSSION

The corrosion fatigue results presented in Figure 3 and the fractographic observations in Figures 4-6 are fully consistent with the residual stress results shown in Figure 2. From previous research, it is generally known that the fatigue strength of surface treated parts is approximately the same as the compressive residual stress. Correspondingly, the surface residual stress of -140 ksi (-965 MPa) and –175 ksi (-1,200 MPa) for the LPB treated specimens correlate quite well with the fatigue strength of LPB treated (unnotched) specimens at a value of about 160 ksi (~1,100 MPa). Similarly, for a 0.010 in. (0.25 mm) deep notch, Figure 3 shows a residual stress in the range of 120 ksi to 150 ksi (~825 to 1035 MPa). The corresponding corrosion fatigue strength is indeed around 125 ksi (~860 MPa). Cutting a deeper notch at 0.020 in. (0.5 mm) depth, the residual stress from Figure 3 shows a value of about –90 ksi (~620 MPa); correspondingly, the two data points for the 0.020 in. deep notch appear to show a tendency towards a fatigue strength of about 90 ksi. Figure 3 shows that at 0.030 (0.75 mm) in deep notch, the residual stress is about –30 ksi (~205 MPa), and correspondingly, the corrosion fatigue performance is expected to be very poor.

These results quite elegantly demonstrate the beneficial effect of surface compressive residual stresses on corrosion fatigue performance.

SUMMARY AND CONCLUSIONS

In summary, the effect of LPB treatment applied to alloy 450 stainless steel (H1050) specimens, tested in corrosion fatigue performance in an acid salt solution environment has been investigated. The effect of EDM notches to simulate pitting and/or FOD related initial damage conditions were studied. The results overwhelmingly indicate that LPB imparted highly beneficial compressive residual stresses on the surface, and further that LPB treated specimens could easily withstand pitting and/or FOD related damage up to a depth of about 0.020 in. (0.5 mm) from the surface. LPB provided a 50% increase in corrosion fatigue strength in the absence of surface damage and a 12x increase in strength for 0.010 in. deep damage. The fatigue strength improvement is attributed to the depth and magnitude of surface compression.

ACKNOWLEDGEMENTS

The authors wish to thank Doug Hornbach for help with residual stress measurements and Perry Mason for his help in conducting fatigue tests.

REFERENCES

1. Frost, N.E. Marsh, K.J. Pook, L.P., *Metal Fatigue*, Oxford University Press, 1974.
2. Fuchs, H.O. and Stephens, R.I., *Metal Fatigue In Engineerin*g, John Wiley & Sons, 1980.
3. Berns, H. and Weber, L., "Influence of Residual Stresses on Crack Growth," Impact Surface Treatment, edited by S.A. Meguid, Elsevier, 33-44, 1984.
4. Ferreira, J.A.M., Boorrego, L.F.P., and Costa, J.D.M., "Effects of Surface Treatments on the Fatigue of Notched Bend Specimens," Fatigue, Fract. Engng. Mater., Struct., Vol. 19 No.1, pp 111-117,1996.
5. Prevéy, P.S. Telesman, J. Gabb, T. and Kantzos, P., “FOD Resistance and Fatigue Crack Arrest in Low Plasticity Burnished IN718”, Proceedings of the 5th National High Cycle Fatigue Conference, Chandler, AZ. March 7-9, 2000.
6. Clauer, A.H., "Laser Shock Peening for Fatigue Resistance," Surface Performance of Titanium, J.K. Gregory, et al, Editors, TMS Warrendale, PA (1996), pp 217-230.
7. P. Prevéy, N. Jayaraman, R. Ravindranath, “Effect of Surface Treatments on HCF Performance and FOD Tolerance of a Ti-6Al-4V Vane,” Proceedings 8th National Turbine Engine HCF Conference, Monterey, CA, April 14-16, 2003
8. Paul S. Prevéy, Doug Hornbach, Terry Jacobs, and Ravi Ravindranath, “Improved Damage Tolerance in Titanium Alloy Fan Blades with Low Plasticity Burnishing,” Proceedings of the ASM IFHTSE Conference, Columbus, OH, Oct. 7-10, 2002

9. Paul S. Prevéy, et. al., "The Effect of Low Plasticity Burnishing (LPB) on the HCF Performance and FOD Resistance of Ti-6Al-4V," Proceedings: 6th National Turbine Engine High Cycle Fatigue (HCF) Conference, Jacksonville, FL, March 5-8, 2001.
10. M. Shepard, P. Prevéy, N. Jayaraman, "Effect of Surface Treatments on Fretting Fatigue Performance of Ti-6Al-4V," Proceedings 8th National Turbine Engine HCF Conference, Monterey, CA, April 14-16, 2003
11. Paul S. Prevéy and John T. Cammett, "Restoring Fatigue Performance of Corrosion Damaged AA7075-T6 and Fretting in 4340 Steel with Low Plasticity Burnishing," Proceedings 6th Joint FAA/DoD/NASA Aging Aircraft Conference, San Francisco, CA, Sept 16-19, 2002
12. N. Jayaraman, Paul S. Prevéy, Murray Mahoney, "Fatigue Life Improvement of an Aluminum Alloy FSW with Low Plasticity Burnishing," Proceedings 132nd TMS Annual Meeting, San Diego, CA, Mar. 2-6, 2003.
13. Paul S. Prevéy and John T. Cammett, "The Influence of Surface Enhancement by Low Plasticity Burnishing on the Corrosion Fatigue Performance of AA7075-T6," Proceedings 5th International Aircraft Corrosion Workshop, Solomons, Maryland, Aug. 20-23, 2002.
14. John T. Cammett and Paul S. Prevéy, "Fatigue Strength Restoration in Corrosion Pitted 4340 Alloy Steel Via Low Plasticity Burnishing," Retrieved Sept. 2, 2003 from http://www.lambda-research.com/publica.htm.
15. Paul S. Prevéy, "Low Cost Corrosion Damage Mitigation and Improved Fatigue Performance of Low Plasticity Burnished 7075-T6", Proceedings of the 4th International Aircraft Corrosion Workshop, Solomons, MD, Aug. 22-25, 2000.
16. Hilley, M.E. ed., (2003), Residual Stress Measurement by X-Ray Diffraction, HS *J784*, (Warrendale, PA: Society of Auto. Eng.).
17. Noyan, I.C. and Cohen, J.B., (1987) Residual Stress Measurement by Diffraction and Interpretation, (New York, NY: Springer-Verlag).
18. Cullity, B.D., (1978) Elements of X-ray Diffraction, 2nd ed., (Reading, MA: Addison-Wesley), pp. 447-476.
19. Prevéy, P.S., (1986), "X-Ray Diffraction Residual Stress Techniques," *Metals Handbook*, **10**, (Metals Park, OH: ASM), pp 380-392.
20. Koistinen, D.P. and Marburger, R.E., (1964), Transactions of the ASM, **67**.
21. Moore, M.G. and Evans, W.P., (1958) "Mathematical Correction for Stress in Removed Layers in X-Ray Diffraction Residual Stress Analysis," SAE Transactions, **66**, pp. 340-345
22. Prevéy, P.S., (1977), "A Method of Determining Elastic Properties of Alloys in Selected Crystallographic Directions for X-Ray Diffraction Residual Stress Measurement," Adv. In X-Ray Analysis, **20**, (New York, NY: Plenum Press, 1977), pp 345-354.